Supporting Information

Plasmonic Bi-doped Bi-$Bi_2Sn_2O_7$/Bi-g-C_3N_4 photothermal catalysis for nitrogen fixation

Lei Zhang,[a,b] Rao Gu,[a] Jianzhong Zhang,[b] Hang Liu,[a] Shien Zhu,[a]

Dawei Su,[c] Tianyi Wang,*[a] Yi Mou*[b] and Chengyin Wang*[a]

[a]*College of Chemistry and Chemical Engineering. Yangzhou University,*

180 Si-Wang-Ting Road, Yangzhou 225002, Jiangsu Province, P.R. China

[b]*College of Pharmacy and Chemistry & Chemical Engineering,, Taizhou University,*

93 Jichuan East Road, Taizhou 225300, Jiangsu Province, P.R. China

[c]*School of Science, STEM College, RMIT University, Melbourne, VIC, 3000, Australia*

Experimental section

Materials

Unless otherwise specified, all reagents are analytically pure and have not been further purified before the experiment. Urea ($CO(NH_2)_2$), Sodium hydroxide (NaOH) and mannitol ($C_6H_{14}O_6$) were purchased from Sinopharm Chemical Reagent Co., Ltd. Polyvinylpyrrolidone ($(C_6H_9NO)_n$), Sodium stannate trihydrate ($Na_2SnO_3 \cdot 3H_2O$), Bismuth oxide (Bi_2O_3) and Stannic oxide (SnO) were purchased from Shanghai Aladdin Biochemical Technology Co., Ltd.

Characterization

The morphological features of materials were observed by using a Zeiss-Supra55 field emission scanning electron microscope and field emission 300 kV high-resolution transmission electron microscopy (HRTEM Tecnai G2 F30 S-TWIN). The samples crystal phases were obtained from X-ray diffraction (XRD Bruker-D8 ADVANCE) with Cu Ka radiation, scan range was 5-80°. In-situ irradiation XPS measurements were conducted using the Thermo Scientific Nexsa G2 instrument equipped with a 405 nm laser. The UV-vis diffuse reflectance spectra (DRS) were recorded on a UV-vis-NIR spectrophotometer (Cary-5000, Varian). The NVs were characterized by electron paramagnetic resonance (EPR) with an A300-10 spectrometer (Bruker, Germany). A nuclear magnetic resonance spectrometer (NMR, Agilent DD2) was used to detect the source of the produced ammonia. The separation efficiency of photocarriers was measured by an Edinburgh FLS920 fluorescence spectrometer. Concentrations of the ammonia were measured with an ultraviolet spectrophotometer (Haineng i5). Elemental analysis was conducted using an organic elemental analyzer (Elementar Vario EL cube, Germany).

Determination of apparent quantum efficiency (AQE). The AQE was obtained by performing N_2 fixation under irradiation from a 300 W xenon lamp combined with different monochromatic filters at wavelengths of 420, 500, 600 and 700 nm respectively. The power intensity of the monochromatic light was measured using an

optical power meter (CEL-NP2000, CEAULIGHT, Beijing). The calculation of AQE was based on:

$$\mathrm{AQE} = \frac{N_{reacted}}{N_{incident}} * 100\% = \frac{3 * N_A * n_{NH_3}}{\frac{pt}{h\nu}} * 100\% = \frac{3 * N_A * n_{NH_3}}{\frac{ISt\lambda}{hc}} * 100\%$$

$N_{reacted}$ is the number of the reacted electrons, n_{NH_3} is the amount of substance for the produced ammonia molecules (mol), N_A is Avogadro constant (6.022×10^{23} mol^{-1}). $N_{incident}$ is the number of the incident photons. *P* is light power (W); *t* is illumination time (s); *h* is Planck constant (6.626×10^{-34} J s); *v* is the light frequency (Hz); *I* is light intensity (W cm^{-2}); *S* is the irradiated area (cm^2); λ is the wavelength of monochromatic light (m); and *c* is the speed of light in free space (3×10^8 m s^{-1}).

Nitrogen isotope labeling experiment

To determine the source of the ammonia produced, $^{15}N_2$ isotope labeling experiments were performed by using a nuclear magnetic resonance spectrometer (NMR, Agilent). First, 25 mg of the catalyst was ultrasonically dispersed in 50 mL of deionized water. The air was removed by continuous passage of Ar (10 mL min^{-1}) for 12 h prior to light exposure. Then $^{15}N_2$ gas was injected into the reactor and the reactor was sealed. The solution was filtered after 12 h of illumination and acidified with sulfuric acid to pH = 2.0. D_2O was subsequently added to the solution for ^1H NMR detection.

Photoelectrochemical measurements

All photoelectrochemical measurements were conducted using an electrochemical workstation (CH Instruments Inc., CHI 660B) in a three-electrode configuration, with a platinum foil as the counter electrode and a saturated Ag/AgCl electrode as the reference electrode. The preparation of the working electrode involved the following steps: 20 mg of the sample, 30 μL of Nafion aqueous solution, and 200 μL of water

were added to 700 μL of isopropanol and ultrasonically dispersed for 30 minutes. Subsequently, 50 μL of the suspension was drop-cast onto an FTO substrate and dried at 60 °C for 6 hours. A 0.5 M Na_2SO_4 solution was used as the electrolyte. The light source illuminated the working electrode from the front side.

Hydrazine detection

N_2H_4 is a common byproduct in nitrogen reduction reactions. In this study, the concentration of N_2H_4 potentially generated during the photocatalytic nitrogen fixation process was monitored using a spectrophotometric method with p-dimethylaminobenzaldehyde (p-DMAB) as the indicator (color reagent), in accordance with the "Environmental Protection Standards of the People's Republic of China" (HJ 674-2013). Prior to the experiment, a series of standard N_2H_4 solutions with varying concentrations were prepared. p-DMAB was added to each solution, thoroughly mixed, and left to stand for 20 minutes. The absorbance was then measured at 458 nm using a UV-Vis spectrophotometer, and a standard calibration curve was established for subsequent concentration determination.

The detection procedure for the reaction solution is as follows: A 5 mL aliquot of the reaction mixture was filtered using a 0.22 μm membrane filter. Subsequently, 0.1 mL of concentrated hydrochloric acid (1.19 g mL^{-1}) was added, and the mixture was diluted to 10 mL with deionized water. From the treated solution, 2.5 mL was taken and mixed with 0.5 mL of p-DMAB. After standing for 20 minutes, the absorbance was measured at 458 nm using a UV-Vis spectrophotometer. The concentration of N_2H_4 produced during the reaction was quantitatively determined by comparing the measured absorbance with the standard calibration curve.

Calculation method:

Colinear spin-polarized density functional theory (DFT) calculations[1, 2] were carried out in the Vienna ab initio simulation package (VASP) based on the plane-wave basis sets with the projector augmented-wave method.[3, 4] The exchange-correlation

potential was treated by using a generalized gradient approximation (GGA) with the Perdew-Burke-Ernzerhof (PBE) parametrization.[5] The energy cutoff was set to be 500 eV. The K-mesh used to sample the Brillouin zone was generated by the VASPKIT[6] and a space sampling interval of less than 0.04 $Å^{-1}$ was chosen to integrate the Brillouin zone with a Γ-centered Monkhorst-Pack mesh[7] in all calculations. The structures were fully relaxed until the maximum force on each atom was less than 0.02 eV/Å, and the energy convergent standard was 10^{-5} eV. To avoid interlaminar interactions, a vacuum spacing of 20 Å is applied perpendicular to the slab. The van der Waals correction of Grimme's DFT-D3 model was also adopted.[8]

The adsorption energy ($E_{ads\text{-}N2}$) is calculated as:

$$E_{ads\text{-}N_2} = E_{heterogeneous@N_2} - E_{heterogeneous} - E_{N_2}$$

where $E_{heterogeneous@N_2}$ is the total energy for heterogeneous with adsorbed N_2, $E_{heterogeneous}$ is the energy for heterogeneous, and E_{N2} is the energy of single N_2.

The biological toxicity test of bismuth-based catalysts

To determine the toxicity of ammonia water fertilizer prepared by photocatalysis, toxicity tests were conducted using Hydrocotyle vulgaris (commonly known as pennywort). The hydroponic experiment was carried out under partial sunlight with temperatures ranging from 15 to 25 °C.

The specific steps of the hydroponic experiment are as follows: 100 mg of Bi-$Bi_2Sn_2O_7$/Bi-CN was dispersed into 200 mL of water. After a 72 h photocatalytic nitrogen fixation reaction, the resulting aqueous solution was filtered. Three pennywort plants were placed in the solution from the nitrogen fixation reaction, and their growth conditions were observed. After 7 days of hydroponic cultivation, the changes before and after were recorded using a camera.

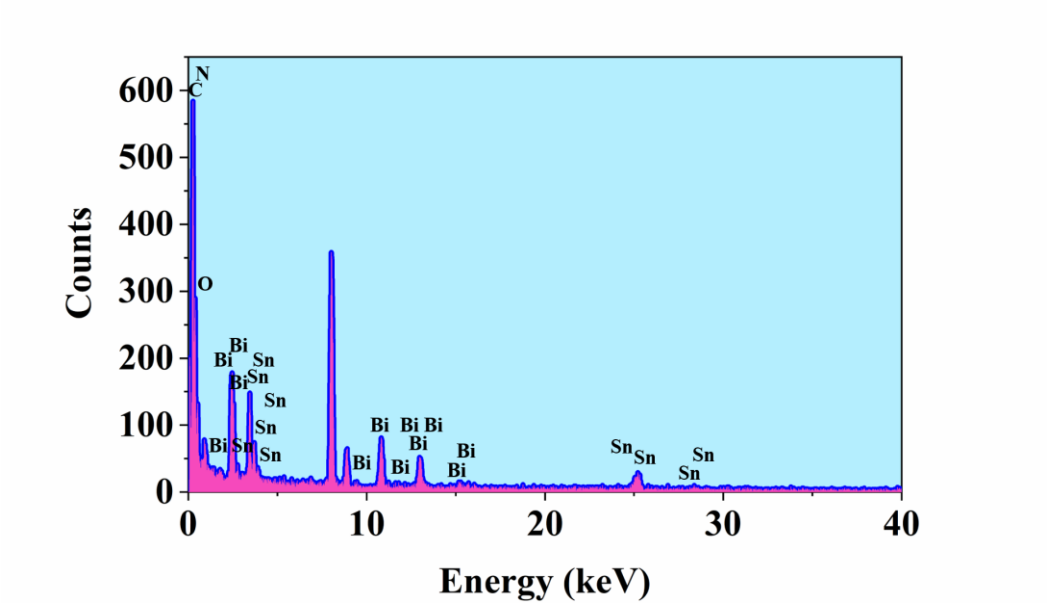

Figure S1. EDX spectrum image of Bi-BiSnO/Bi-CN.

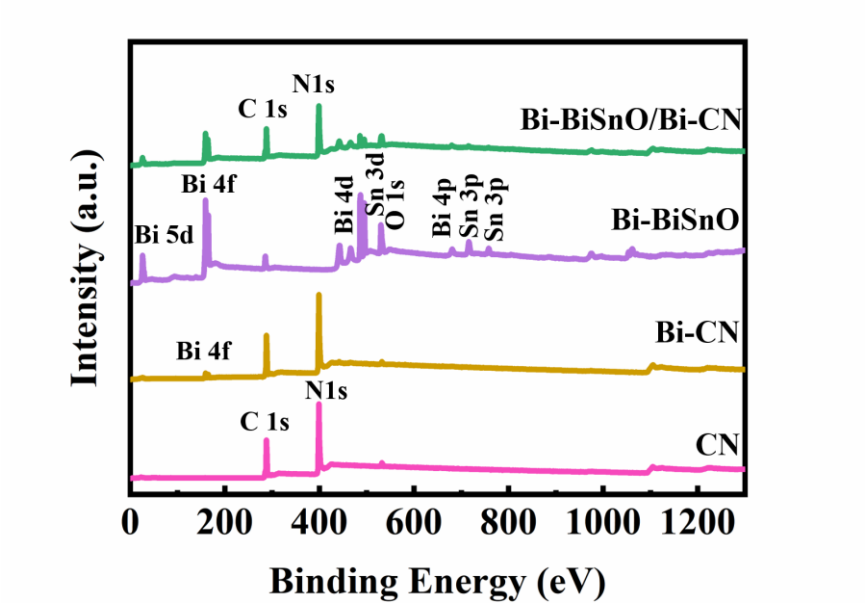

Figure S2. The XPS survey spectrum of CN, Bi-CN, Bi-BiSnO and Bi-BiSnO/Bi-CN.

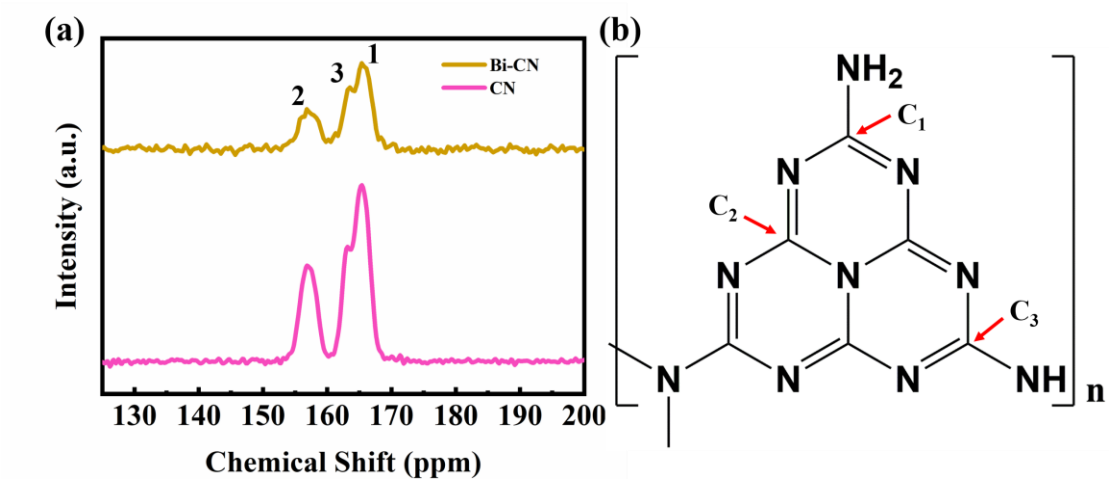

Figure S3. Solid-state MAS ^{13}C NMR spectra of the CN and Bi-CN samples.

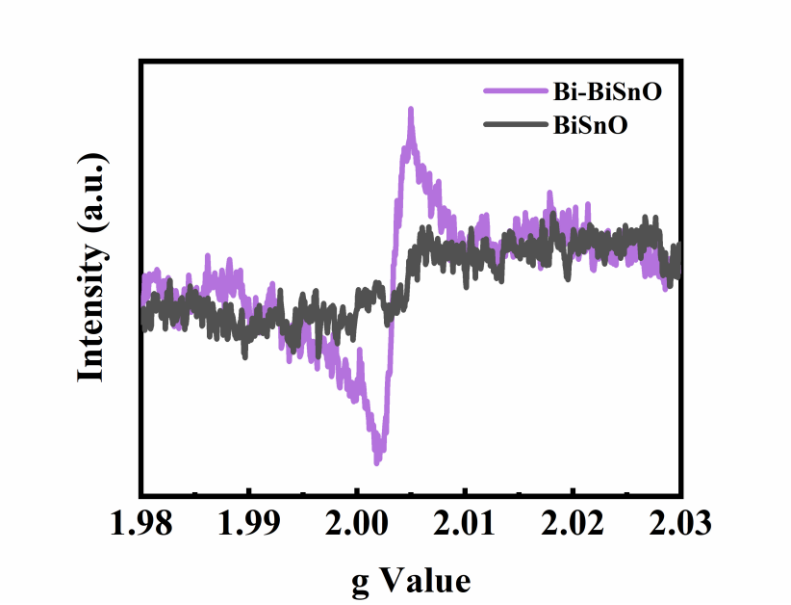

Figure S4. EPR spectra of CN and Bi-CN.

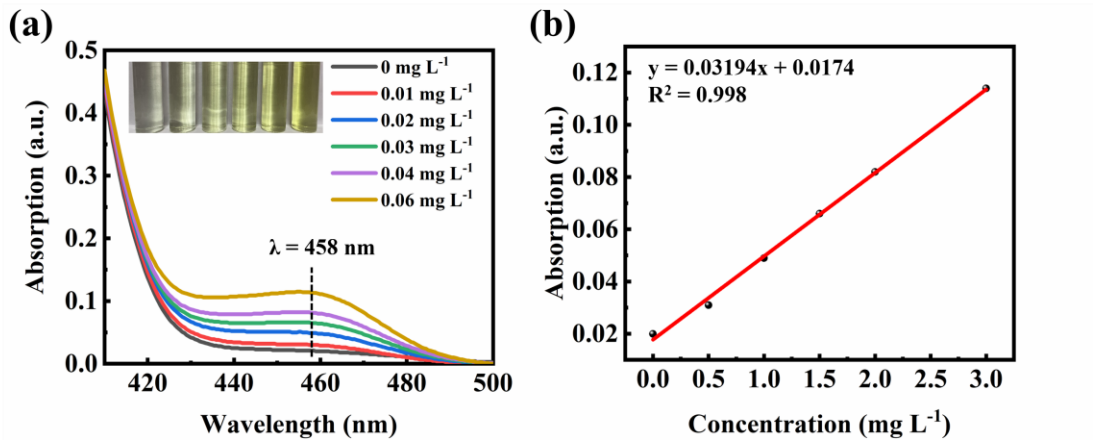

Figure S5. (a) Absorbance spectra of $N_2H_4 \cdot H_2SO_4$ stand solutions, and (b) the corresponding calibration curve for $N_2H_4 \cdot H_2SO_4$.

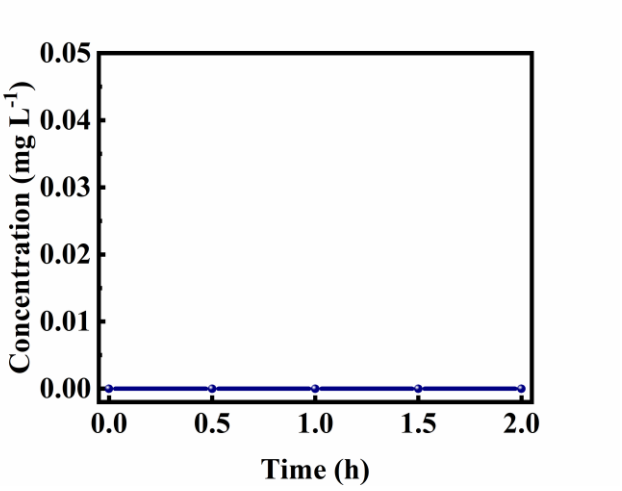

Figure S6. Determination of N_2H_4 content during the Bi-BiSnO/Bi-CN photocatalytic nitrogen fixation process using the p-dimethylaminobenzaldehyde spectrophotometric method.

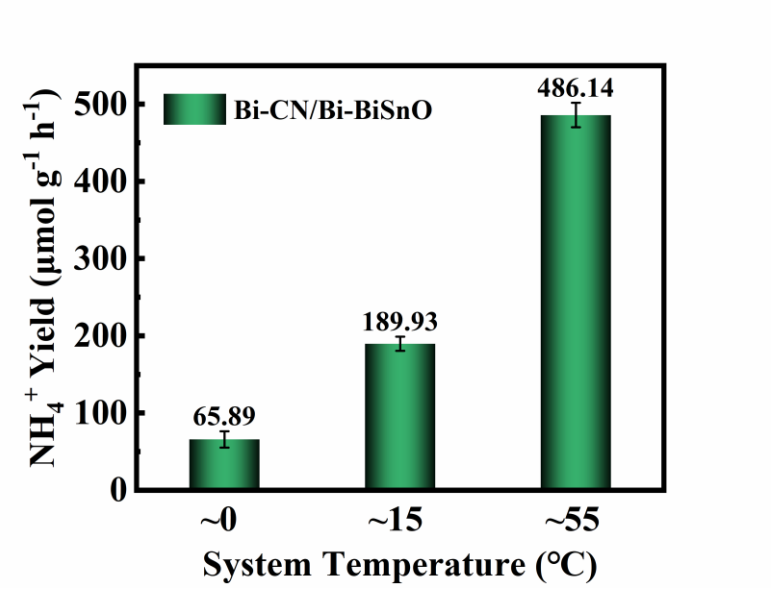

Figure S7. Comparison of nitrogen fixation efficiencies at different temperatures using Bi-CN/Bi-BiSnO as the photocatalyst.

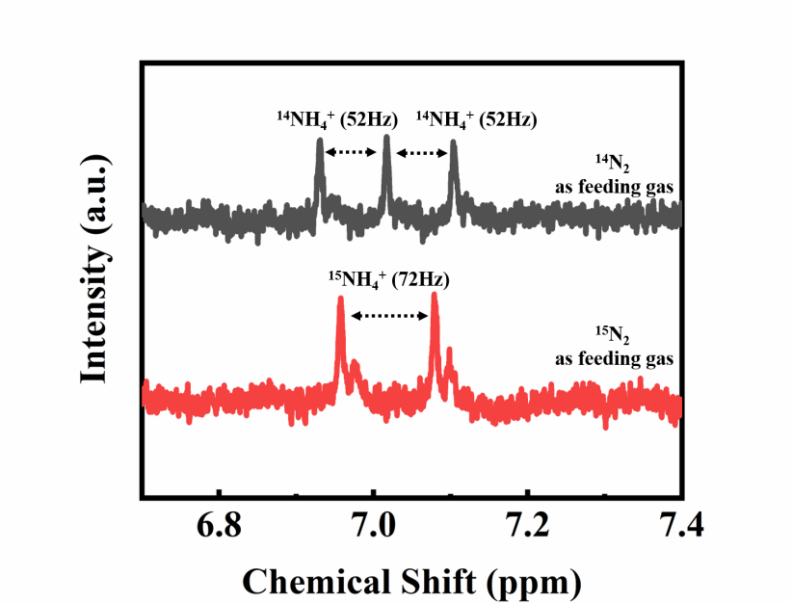

Figure S8. ^{1}H NMR results of photocatalytic reduction mediums under $^{15}N_2$ and $^{14}N_2$ atmosphere, respectively.

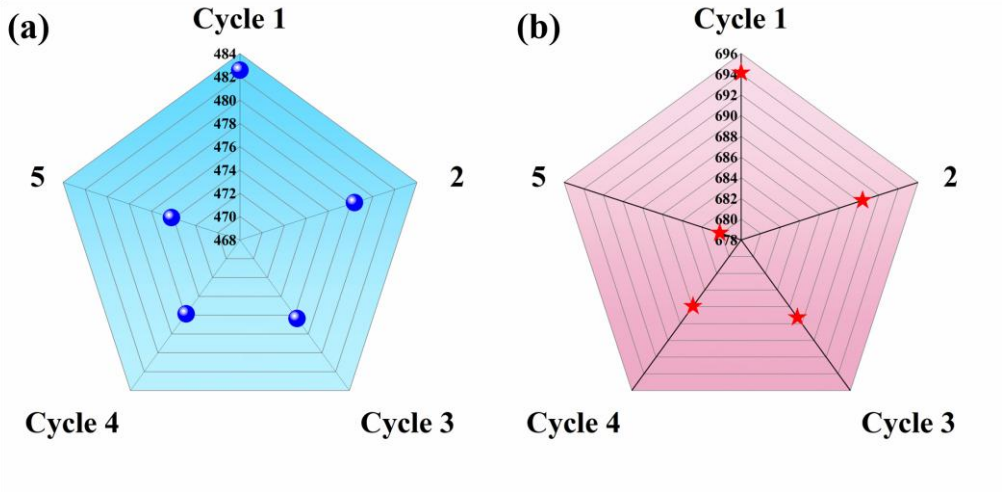

Figure S9. The cycling numbers of $Bi_2Sn_2O_7$/Bi-CN for photo-thermal catalytic nitrogen fixation upon (a) visible light and (b) full spectrum.

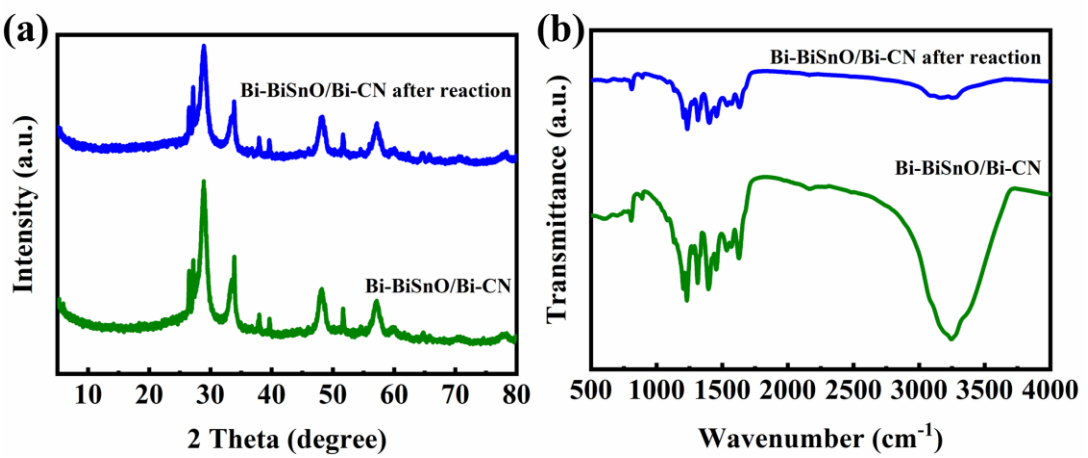

Figure S10. (a) XRD spectrum and (b) IR spectrum of $Bi_2Sn_2O_7$/Bi-CN after reaction.

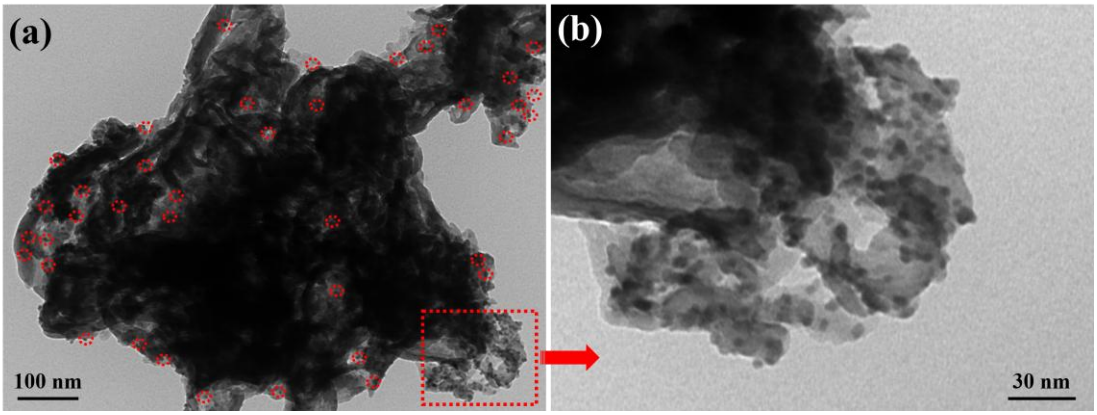

Figure S11. TEM images of $Bi_2Sn_2O_7$/Bi-CN after reaction.

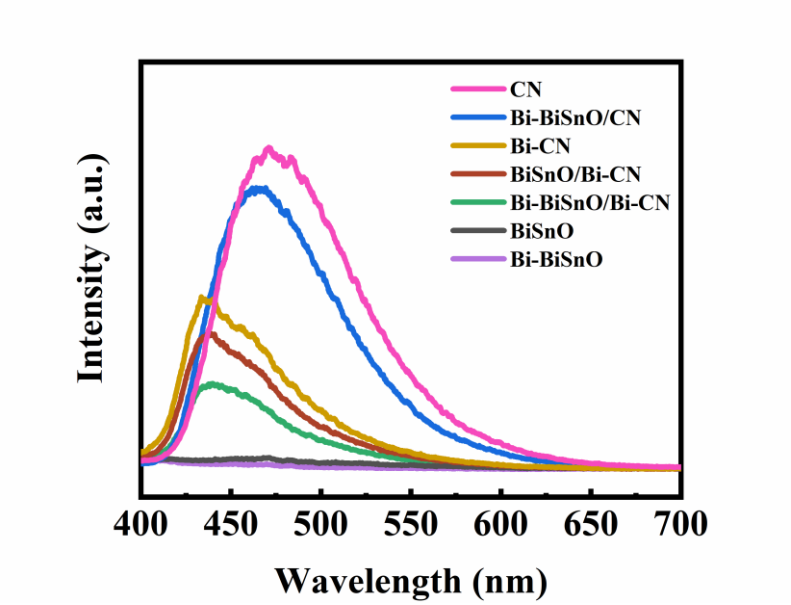

Figure S12. Steady photoluminescence of different photocatalysts.

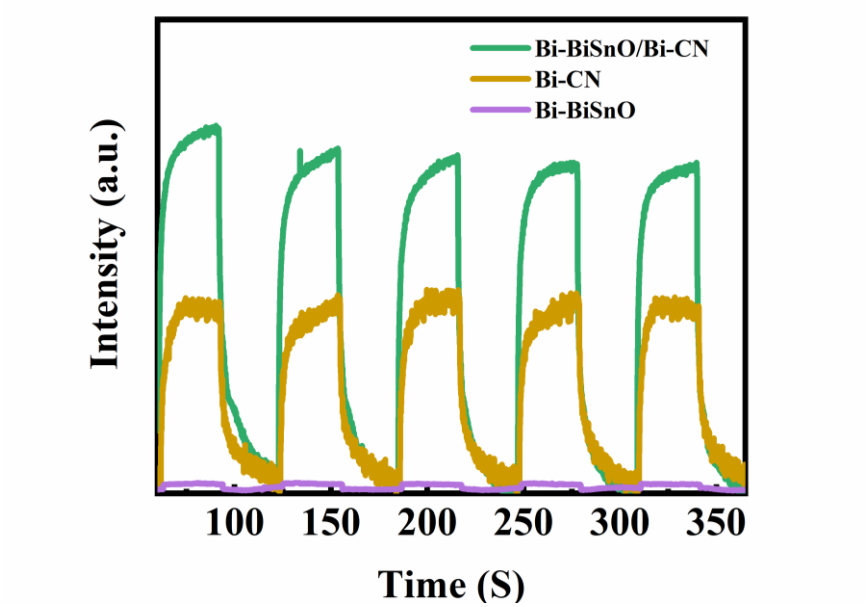

Figure S13. Photocurrent of different photocatalysts.

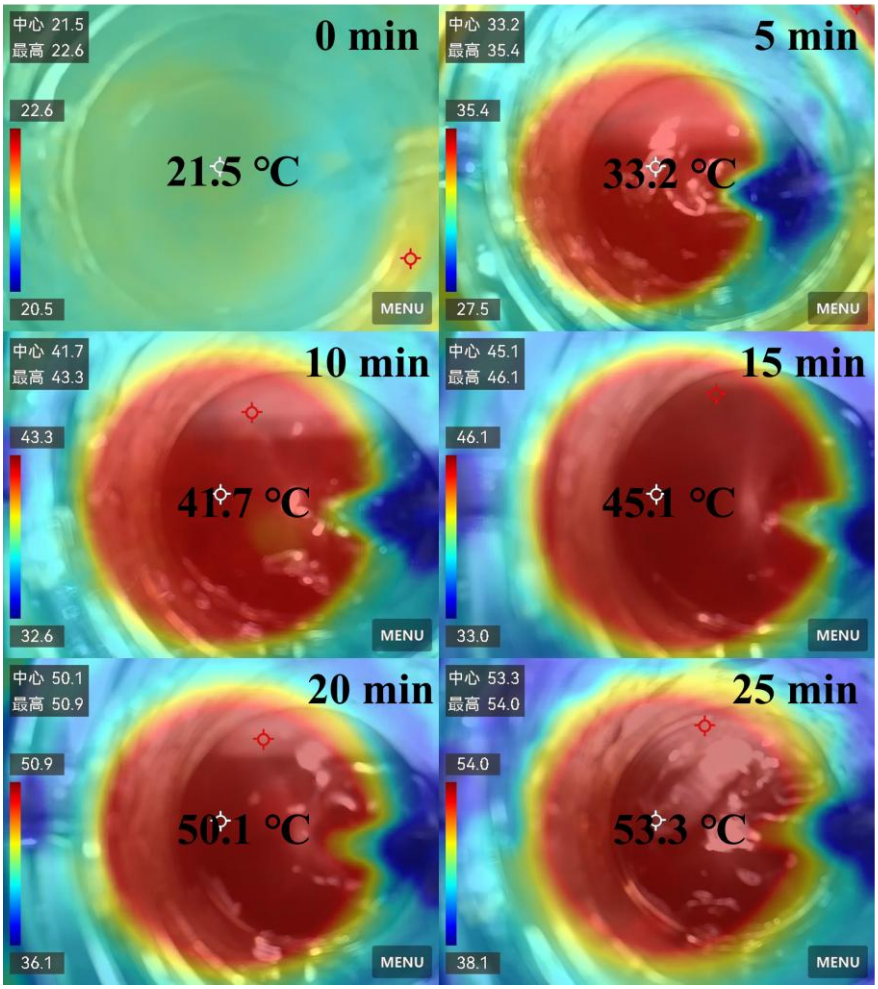

Figure S14. The IR images of vertical view under 300 W Xe lamp illumination for different times recorded on IR thermal camera.

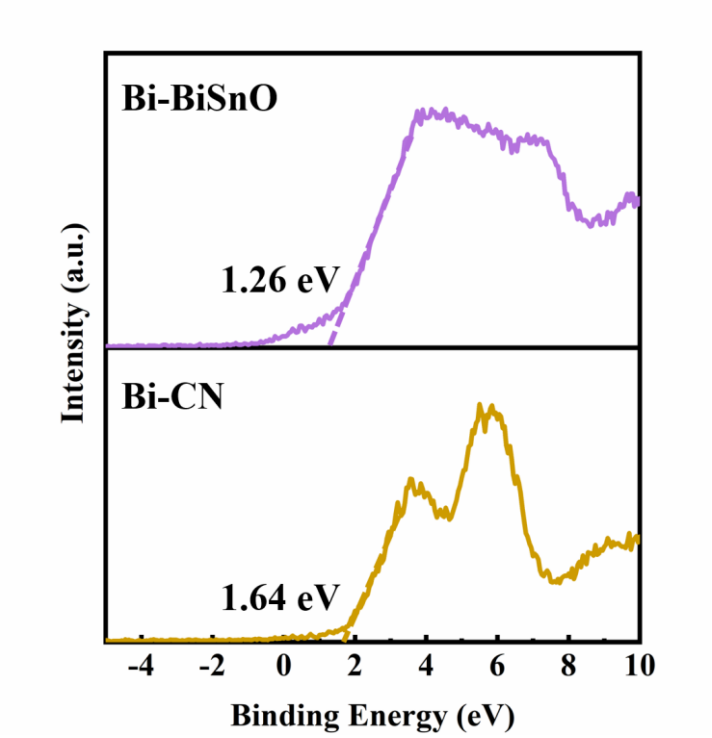

Figure S15. XPS VB spectra of different samples.

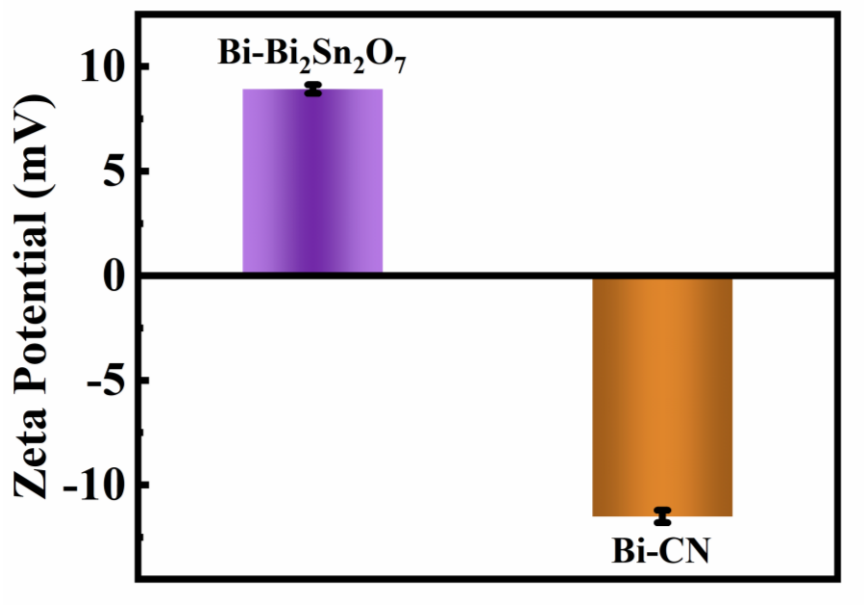

Figure S16. Zeta potential of $Bi_2Sn_2O_7$ and Bi-CN in aqueous solution.

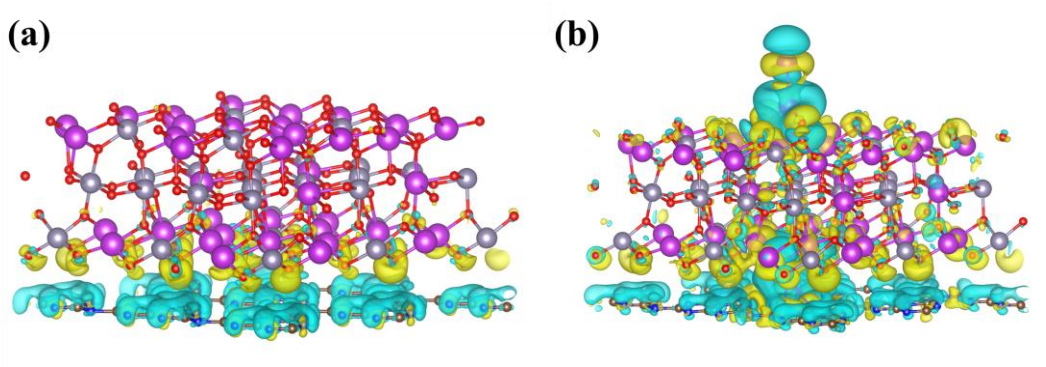

Figure S17. Differential charge density mappings of (a) CN/BiSnO and (b) Bi-CN/Bi-BiSnO (the yellow regions represent electron accumulation, while the green regions indicate electron depletion).

Table S1. Atomic ratio of Bi-CN, Bi-BiSnO, Bi-CN/Bi-BiSnO (dark) and Bi-CN/Bi-BiSnO (light) determined by XPS.

Catalyst	Percent of C (%)	Percent of N (%)	Percent of O (%)	Percent of Bi (%)	Percent of Sn (%)
Bi-CN	56.26	40.57		0.23	
Bi-BiSnO			39.47	7.84	8.42
Bi-CN/Bi-BiSnO (dark)	41.03	47.51	9.3	1.46	0.69
Bi-CN/Bi-BiSnO (light)	43.29	46.11	8.5	1.42	0.68

Table S2 Basic indexes and limits of drinking water, surface water and farmland irrigation water

Item	Drinking water limit values	Class V Surface Water Limits	Limits for Farmland Irrigation Water
Total Lead	10	100	200
Total cadmium	5	10	10
Cr (Hexavalent)	50	100	100
Total Arsenic	10	100	50
Bismuth	Not specified	Not specified	Not specified

Note: Class V is primarily suitable for agricultural water areas and general landscape water bodies; for farmland irrigation water, the types of crops are paddy crops.

Table S3 The concentration of bismuth precipitated in photocatalysts

Photocatalysts	Reaction time	Element	Concentration ppb (μg L^{-1})
Bi-$Bi_2Sn_2O_7$/Bi-g-C_3N_4	24 h	Bi	3.2
	48 h	Bi	3.2
	72 h	Bi	3.3

Table S4. Selected results for catalytic N_2 fixation in recent literature.

Photocatalyst	Light source (nm)	scavenger	Ammonia production rate ($\mu mol\ h^{-1}\ g_{cat}^{-1}$)	Refs.
Bi-$Bi_2Sn_2O_7$/Bi-CN	400-780	None	486.14	**This work**
Bi-$Bi_2Sn_2O_7$/Bi-CN	300-2500	None	699.76	**This work**
Au/Rh	λ > 420 nm	methanol	138.2	J. Am. Chem. Soc. 146 (2024) 7734-7742
Bi@ZnCdS	300 W Xe lamp	None	58.93	Inorg. Chem. 63 (2024) 5065-5075
Cu_2O-$W_{18}O_{19}$	AM 1.5G	None	252.4	Small 20 (2024) 2306229
Fe/$Bi_2O_{2.33}$	300 W Xe lamp	None	118.71	J. Colloid Interface Sci. 661 (2024) 46-58
g-C_3N_4/COF	λ > 420 nm	None	238.1	Fuel 358 (2024) 130157
$Ti_3C_2O_x$/MIL-125(Ti)	320-780 nm	None	103.2	Appl. Catal., B 346 (2024) 123732
Ce/S-TiO_2	λ > 420 nm	None	382.4	J. Mater. Chem. A 12 (2024) 7163
MIL-125(Ti)	320-780	None	156.9	Angew. Chem. Int. Ed. 63 (2024) 202316973
OVs-$BaTiO_3$	AM 1.5G	Sodium sulfite	106.7	Adv. Mater. 36 (2024) 2303845

References:

1 Hohenberg, P. & Kohn, W. Inhomogeneous Electron Gas. *Physical Review*, 1964, **136**, B864-B871.

2 Kohn, W. & Sham, L. J. Self-Consistent Equations Including Exchange and Correlation Effects. *Physical Review*, 1965, **140,** A1133-A1138.

3 Kresse, G. & Furthmüller, J. Efficient iterative schemes for ab initio total-energy calculations using a plane-wave basis set. *Physical review B*, 1996, **54**, 11169.

4 Blöchl, P. E. Projector augmented-wave method. *Physical Review B*,1994, **50**, 17953-17979.

5 Perdew, J. P., Burke, K. & Ernzerhof, M. Generalized gradient approximation made simple. *Physical Review Letters*, 1996, **77**, 3865.

6 Wang, V., Xu, N., Liu, J.C., Tang, G., Geng, W.T. VASPKIT: A user-friendly interface facilitating high-throughput computing and analysis using VASP code. *Computer Physics Communications*. 2021, **267**, 108033.

7 Monkhorst, H. J. & Pack, J. D. Special points for Brillouin-zone integrations. *Physical Review B*, 1976, **13**, 5188-5192.

8 Grimme, S., Antony, J., Ehrlich, S. & Krieg, H. A consistent and accurate ab initio parametrization of density functional dispersion correction (DFT-D) for the 94 elements H-Pu. *The Journal of Chemical Physics*, 2010, **132**, 154104.